eProceedings Chemistry 3 (2018) 56-63

eISSN 2550-1453 http://eproceedings.chemistry.utm.my/

Statistical optimization of *Candida rugosa* lipase supported on chitosan/nanocellulose composite for efficient synthesis of butyl butyrate

Mohamad Faqehuddin Mohd Razib, and Roswanira Abdul Wahab*

Department of Chemistry, Faculty of Science, Universiti Teknologi Malaysia, 81310 Johor Bahru, Malaysia
Corresponding Author: roswanira@kimia.fs.utm.my

Article history:
Received 3 Oct 2018
Accepted 21 Nov 2018

GRAPHICAL ABSTRACT

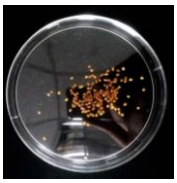

Immobilized CS/NC-CRL beads

ABSTRACT

Current commercial route to synthesize butyl butyrate (BuBu) using acid catalyst tend to produce unwanted byproducts that are detrimental to human health and environment. In this perspective, the alternative biotechnological pathway using immobilized *Candida rugosa* lipase (CRL) onto solid support may be a feasible solution. In this study, the raw oil palm frond leaves (OPFL) was treated with three different kinds of chemical treatments including bleaching, alkaline treatment, and acid hydrolysis to obtain the purified nanocellulose (NC). The extracted NC was then used as nano-filler to develop the stable chitosan (CS)/NC hybrid supports to immobilize CRL to produce CS/NC-CRL biocatalyst. The approach of Response Surface Methodology (RSM) using a 3-level-3-factor Box-Behnken design (time, temperature, and concentration of crosslinker) was used to optimize the immobilization protocol of CS/NC-CRL, based on the highest percentage yield of synthesized BuBu. Substantially, the developed CS/NC-CRL biocatalyst here can act as a promising environmentally friendly biocatalyst as compared to the homogenous acid catalyst in the high yield production of BuBu.

Keywords: Candida rugosa lipase, nanocellulose, butyl butyrate, immobilization protocol

1. INTRODUCTION

The difficulty associated with removal of large quantities of agricultural biomass from the ecosystem is a global concern. The abundance of post-harvest agricultural lignocellulosic biomass dumped in the environment to decompose naturally is a challenge faced by many nations throughout the globe (Anwar *et al*., 2014). In light of this, this study therefore, focuses on finding an alternative avenue to effectively convert the abundant oil palm biomass into value-added products (Aljuboori *et al*., 2013).

Oil palm is highly rated amongst the oil producing crops. However, cultivation of this highly valued crop has left so much biomass waste in the nations where it is cultivated in large quantities. Commonly, there are three primary classifications of oil palm biomass which are empty fruit bunches (EFB), oil palm frond leaves (OPFL) and oil palm trunk (OPT). Precisely, oil palm solid biomass comprises of three primary biopolymers which include cellulose (~30-50% wt), hemicelluloses (~19-45% wt) and lignin (~15-35% wt) (Lee *et al*., 2014). It is abundantly available of solid agro waste on oil palm plantations.

CS is known relatively low stability of enzyme in their native state (Sarbon *et al*., 2015). Pertinently, cellulose and CS were chosen in this study for developing a novel support for immobilizing lipases because of their biocompatibility, biodegradability and non-toxicity (Pillai *et al*., 2009) as well as possessing high adsorption capacity (Dash *et al*., 2011). Cellulose, $(C_6H_{10}O_5)_n$ is an organic compound from polysaccharide family that comprises of a straight chain of D-glucose units linked by ß-1,4 glycosidic bond (Yahya *et al*., 2015). Awalludin *et al*. (2015) stated that Malaysia being among the largest producers of palm oil in the world has numerous large-scale plantations that generate large amounts of this biomass waste estimated over 190 million tons in 2015. The extracted palm oil only accounts for ~ 10% of the processed oil palm fruit bunch while the remaining 90% of the biomass is treated as waste in most cases. The abundant neglected and unwanted oil palm biomass in Malaysia may prove to be a good as well as renewable source of NC to produce environmentally friendly value-added products.

Lipase (triacylglycerol acylhydrolase) is regarded as one of the most essential and extensively used enzyme, particularly for industrial and analytical chemistry applications (Elhakeem *et al*., 2014). Among the readily available commercial lipases in the market, *Candida rugosa* lipase (CRL) has been chosen in this study due to the myriad of reactions it is capable of catalyzing, both in aqueous and nonaqueous media (Hung *et al*., 2003). According to Marzuki *et al*. (2015), CRL in its free form is unstable and is easily deactivated under prolonged exposure to extreme conditions *viz.* pH and high temperature. The enzyme also exhibits low activity in organic solvents. Elhakeem *et al*. (2014) suggested that their selectivity, operational stability and activity can be modified by their

immobilization onto a solid support. This approach is typically adopted to facilitate more efficient utilization of the biocatalyst, in conjunction to averting premature destabilization of the lipase.

The efficacy of CS/NC-CRL nanobiocatalysts is appraised for catalyzing an esterification reaction. In this investigation, the reaction utilized is esterification of butanol and butyric acid to butyl butyrate. This reaction is of prime interest of the study considering its poor yield of the target ester, as well as the energy intensive commercial process, in which can be better improved for cost-effectiveness. Essentially, the current commercial Fisher-Speier method to produce butyl butyrate has several drawbacks such as the utilization of corrosive acid catalysts, production of dangerous by products, complex separation processes and harsh reaction conditions (Ju *et al*., 2011). Additionally, the use of high reaction temperatures (200-250˚C) also cause 50% of the formed butyl butyrate to be degraded (Ju *et al.* 2011). Therefore, exploring a more robust and greener technique via the biotechnological route becomes significant. These issues pertaining to the synthesis of butyl butyrate can be circumvented via the biotechnological approach. This is because the enzyme-assisted esterification typically occurs under ambient conditions while being an environmentally desirable technique. The use of CRL immobilized onto CS/NC hybrid support (CS/NC-CRL) is also comparably greener than the chemically-assisted synthetic route employed in the industry.

2. EXPERIMENTAL

The experiment was divided into three main steps which include extraction of nanocellulose from oil palm frond leaves (OPFL), optimization of the immobilization protocol using response surface methodology (RSM), and lastly the purification and analysis of the enzymatic reaction product i.e. butyl butyrate. In order to extract the NC, OPFL was sorted, cleaned, cut, and dried into finer sizes before undergoing three different kinds of chemical treatments including bleaching, alkaline treatment, and acid hydrolysis to obtain the purified NC. The raw OPFL and extracted NC were then characterized using Fourier-Transform Infrared (FTIR), and X-Ray Diffraction (XRD) to study the biochemical and morphological characteristics of the extracted NC. In the second steps, RSM was utilized to perform the immobilization of 20 mL free CRL (10 mg/mL) onto CS/NC beads at three different parameters which include time, temperature, and concentration of crosslinker, gluteraldehyde. The suitability of each step of the immobilization protocol was based on the yield of butyl butyrate catalyzed by the CS/NC-CRL biocatalysts. Later in the last step, the developed CS/NC-CRL was used to synthesize butyl butyrate. The reaction mixtures were pooled and purified by distillation technique. The pure butyl butyrate obtained was confirmed using FTIR and Nuclear Magnetic Resonance (NMR).

3. RESULTS AND DISCUSSION

3.1 Extraction and characterization of NC

The extraction of NC from OPFL involved three different chemical treatments *viz.* chlorite bleaching, alkali treatment, and acid hydrolysis. The resultant NC was obtained after centrifugation of the NC suspension in distilled water to remove the excess acid.

The peak intensities of XRD (Figure 1) for raw OPFL and NC presented a monoclinic sphenodic structural characteristic of Cellulose-I polymorph, which strongly implied the pretreatment of raw OPFL does not significantly influence the natural Cellulose-I structure. From the graph, it can be seen that intensities of peaks at $2\theta = 15^{\circ}$ and $2\theta = 22^{\circ}$ were slightly increased after the chemical pretreatments. The peak for the extracted NC showed good definition reflected in the greater lattice peak which indicates the NC is higher crystallinity than the raw OPFL.

The FTIR spectrum of NC was represented in Figure 2. The appearance of prominent broad band of NC at the frequency of 3291.09 cm^{-1} denotes the O-H stretching vibration with contribution of the N-H group stretching. The peaks that appeared at frequency 1569.08 cm^{-1} and 1374.89 cm^{-1} shows the presence of amide I and amide II allotted to an absorbance of glucosidic bond, stretching vibration from C=O of –NHCO. The peak at frequency 1027.13 cm^{-1} assigned to the C-O stretching from the deacetylation of CS resulting in the presence of multiple C-O bonds in oxygen bridges.

Figure 3 illustrates the TGA and DTG curves for decomposition of CS, NC, CS/NC and CS/NC-CRL and tabulated data in Table 1. Based on the thermogram, all of the sample showed an initial small weight loss between 50 °C to 100 °C (~2 - 5%) corresponding to the evaporation of bounded water on the surface of the support. Interestingly, with the profile of degradation of NC showed two patterns. A mass loss observed around 100 - 300 °C

(32%) and 300 - 500 °C (31%) was due to thermal decomposition of hemicellulose and lignin as well as pyrolysis of cellulose, respectively.

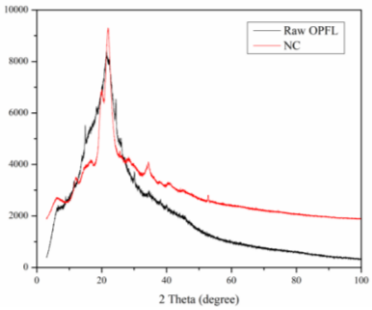

Figure 1 X-ray diffraction patterns of the raw OPFL and NC.

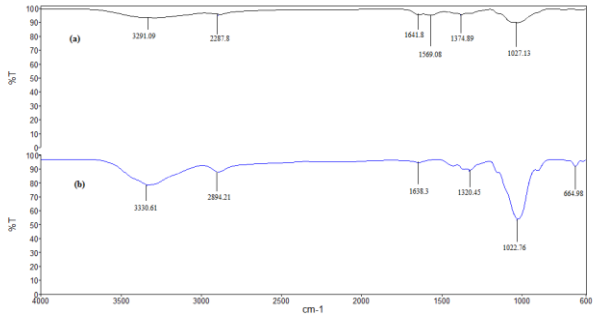

Figure 2 FTIR spectra for a) CS b) NC.

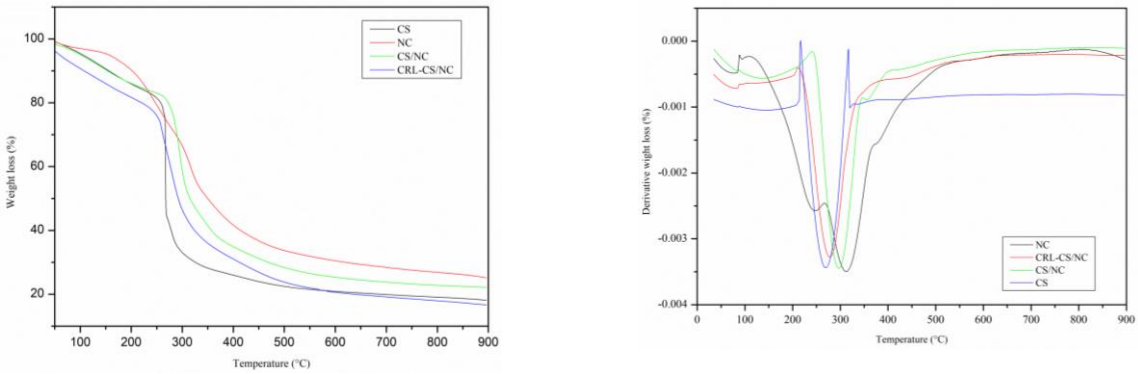

Figure 3 Thermogram of TGA and DTG of CS, NC, CS/NC and CS/NC-CRL.

3.2 Optimization of Immobilized Protocol using Response Surface Methodology

The produced CRL-CS/NC biocatalyst was used to catalyze the esterification synthesis of BuBu from unmodified butanol and butyric acid. The operating condition for the reaction was investigated with the use of Response Surface Methodology (RSM). It this assessment the influence of time (A), temperature (B), and concentration of crosslinker (C) to afford the highest percentage of BuBu. The RSM used a Box-Behnken Design (BBD) for the fitting a second-order response surface. This model analyzed various parameters including P-value, F-value, lack of fit of model, coefficient of determination (R^2), adjusted coefficient of determination (R_{adj}^2), and standard deviation to reproduce the statistical significance of the developed quadratic model.

The result of the RSM using BBD (Table 1) disclosed that the condition of (time: 5h, temperature: 30˚C, and concentration of crosslinker: 0.30%) was the most efficient because it gave the highest actual yield of BuBu (77.38%). Conversely, the lowest actual yield of BuBu (15.58%) was at the condition of (time: 5 h, temperature: 4˚C, and concentration of crosslinker: 0.30%) showing that the reaction is not efficient.

Table 1 BBD with the actual and predicted values for percentage of BuBu

Run	Time (h)	Temperature (°C)	Concentration of crosslinker (%)	Actual (%)	Predicted (%)
1	5 (0)	17 (0)	1.65 (0)	50.96	53.79
2	2 (-1)	17 (0)	3.00 (1)	59.57	62.90
3	5 (0)	4 (-1)	3.00 (1)	55.66	59.43
4	5 (0)	17 (0)	1.65 (0)	48.76	53.79
5	2 (-1)	17 (0)	0.30 (-1)	62.23	66.98
6	5 (0)	30 (1)	3.00 (1)	39.49	35.14
7	2 (-1)	4 (-1)	1.65 (0)	56.08	57.99
8	8 (1)	17 (0)	0.30 (-1)	50.47	53.15
9	5 (0)	30 (1)	0.30 (-1)	77.38	80.61
10	8 (1)	30 (1)	1.65 (0)	65.36	63.45
11	5 (0)	17 (0)	1.65 (0)	51.88	53.79
12	8 (1)	17 (0)	3.00 (1)	49.01	51.26
13	5 (0)	4 (-1)	0.30 (-1)	15.58	19.93
14	5 (0)	17 (0)	1.65 (0)	56.33	53.79
15	5 (0)	17 (0)	1.65 (0)	49.04	53.79
16	2 (-1)	30 (1)	1.65 (0)	68.32	72.34
17	8 (1)	4 (-1)	1.65 (0)	37.43	41.41

The value of predicted and actual yields (Figure 4) correlated well (R^2 = 0.9848) indicated that the generated model appears reliable and could yield good prediction of the best immobilization conditions to obtain the most activated CS/NC-CRL to catalyze the highest production of BuBu.

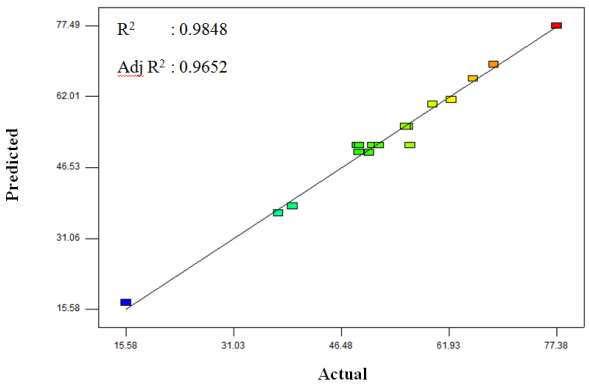

Figure 4 Comparison of predicted response of BuBu percentage yield with experimental response.

Based on data of analysis of variance (ANOVA) (Table 2), the variable, immobilization temperature, B (p value < 0.0001, F value 139.93) was seen to have the most impact in producing the best CRL-CS/NC to yield the highest amount of BuBu, followed by the effect of immobilization time, A (p value < 0.0005, F value 36.68).

Table 2 also indicated that most of the total variation in the experimental data can be explained by the model including the independent variables A (p value = 0.0005) and B (p value < 0.0001) were all significant (p value < 0.05) except for C (p value 0.7978). In addition, two out of three mutual interactions were also significant (AB: time x temperature; BC: temperature x concentration of crosslinker).

Table 2 Analysis of variance table of the BBD

Source	Sum of square	df	Mean Square	F value	p value Prob > F	
Model	2975.16	9	330.57	50.27	< 0.0001	significant
A-Time	241.23	1	241.23	36.68	0.0005	
B- Temperature	920.20	1	920.20	139.93	< 0.0001	
C- Concentration of crosslinker	0.47	1	0.47	0.071	0.7978	
AB	61.54	1	61.54	9.36	0.0183	
AC	0.36	1	0.36	0.055	0.8217	
BC	1519.83	1	1519.83	231.11	<0.0001	
A^2	197.45	1	197.45	30.02	0.0009	
B^2	8.79	1	8.79	1.34	0.2857	
C^2	35.95	1	35.95	5.47	0.0520	
Residual	46.03	7	6.58			
Lack of Fit	8.77	3	2.92	0.31	0.8160	not significant
Pure Error	37.27	4	9.32			
Cor Total	3021.20	16				

3.3 Impact of Immobilization Variables towards Synthesis of Butyl Butyrate (BuBu)

The effects of time (A), temperature (B), and oncentration of crosslinker (C) on synthesis of BuBu were compared using the perturbation plot as shown in Figure 5. From the graph, the yield of BuBu increases significantly as B increases, giving B, supporting the data of ANOVA showing, immobilization temperature B being the most influential parameter. From Figure 5, B was seen to increase tangentially throughout the process, indicative of the dependence of the immobilization protocol on temperature. The lowest percent yield of BuBu was observed for the CS/NS-CRL immobilized at 4˚C. Whereas CS/NS-CRL immobilized at the highest temperature (30 ˚C) gave the highest percentage of BuBu. The parameter C (concentration of the crosslinker) has least effect to improve percent synthesis of BuBu.

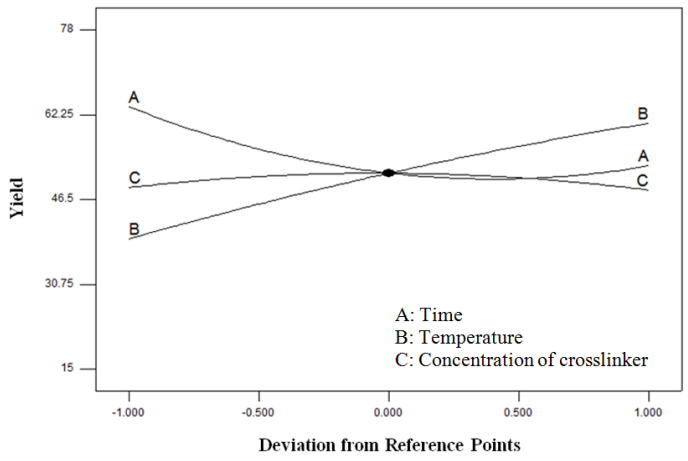

Figure 5 The deviation from reference point for the percentage yield of BuBu for the effects of A) Time, B) Temperature, and C) Concentration of crosslinker.

3.3.1 Effect of Time and Temperature

Figures 6 (a) and (b) illustrated the contour and surface plots for the mutual interaction of time (A) and temperature (B) to determine the immobilization parameters efficient in producing the best CS/NC-CRL to catalyze the highest synthesis of BuBu, respectively. As can be seen, their interaction was significant (F value 9.36; p value 0.0183). Based on the contour plot (Figure 6 (a)), it was shown that the highest percentage yield of BuBu can be achieved when the CRL immobilization temperature is set at 30˚C with a 5 h immobilization time. Conversely, the lowest percentage yield of BuBu was observed when an immobilization temperature and time of 4˚C and 5 h were used, respectively. Interestingly, the contour plot revealed that the highest percent of BuBu at 67.54 could be achieved using the highest immobilization temperature (30˚C) and immobilization time (8 h) or the highest immobilization temperature at the shortest immobilization time (2 h).

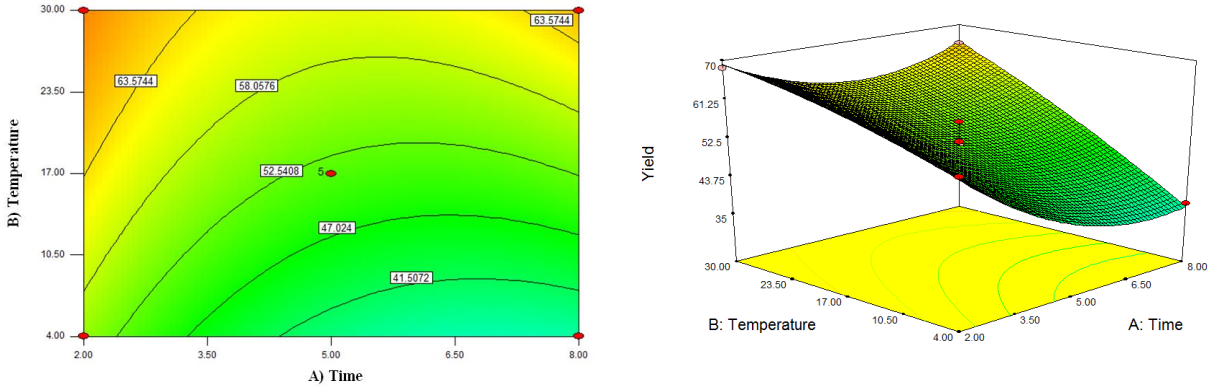

Figure 6 The a) contour plot and b) surface plot of mutual effect between temperature and time, AB.

3.3.2 Effect of Temperature and Concentration of Crosslinker

Figures 7 (a) and (b) illustrated the contour and surface plots for the mutual interaction of temperature (B) and concentration of crosslinker (C) to affect the immobilization efficiency to give the highest percent of BuBu, respectively. It can be seen that the effect of temperature was more significant than the concentration of crosslinker, by comparison of their F values. Based on the contour plot in Figure 7 (a), it was shown that the highest percentage yield of BuBu can be achieved when the CRL immobilization temperature was set at its highest at 30˚C, while glutaraldehyde is held at the lowest concentration of 0.30% (v/v). In contrast, the lowest percentage of BuBu was achieved with the immobilization temperature set to lowest at 4˚C using 0.30% (v/v) of glutaraldehyde.

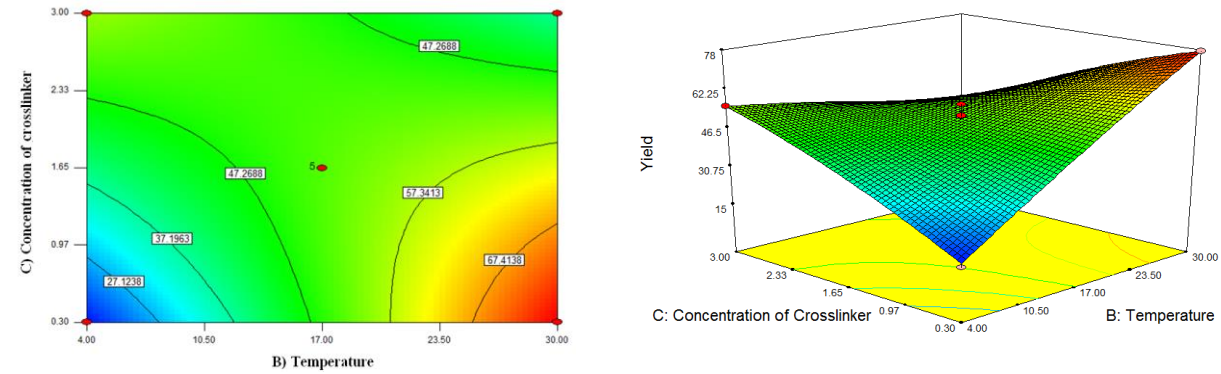

Figure 7 The a) contour plot and b) surface plot of mutual effect between concentration of crosslinker and temperature, BC.

3.4 Purification and analysis of butyl butyrate

In this study, to confirm butyl butyrate was the main product of the esterification reactions catalyzed by the CRL-CS/NC, the reaction mixtures were pooled and purified by distillation technique and was identified using Fourier-Transform Infrared (FTIR), and Nuclear Magnetic Resonance (NMR).

3.4.1 FTIR Spectroscopy: Attenuated Total Reflectance (FTIR-ATR)

The purified BuBu was analyzed using FTIR-ATR. The spectrum of the purified BuBu produced by CS/NC-CRL is portraying in Figure 8. The absorption band at frequency 2924.10 cm^{-1} refers to asymmetric and symmetric stretching vibrations of C-H sp^3. The absorption band at frequency 1713.40 cm^{-1} assigned to the C=O of ester. The result shows that BuBu was successfully synthesized by the CS/NC-CRL. The peak at frequency 1184.90 cm^{-1} – 1051.00 cm^{-1} can be assigned to the stretching vibration of C-O ester as the correlation table of FTIR shows that the region for C-O is 1000 cm^{-1} - 1300cm^{-1}. A peak that appeared at frequency 1456.20 cm^{-1} is the stretching vibrations for the sp^3 of –C–H (alkane) bonding. A slightly broad peak in the region of 3200 cm^{-1} was likely due to minute amounts of butanol. This indicates the purification protocol *via* the use of distillation was not capable to remove all traces of butanol.

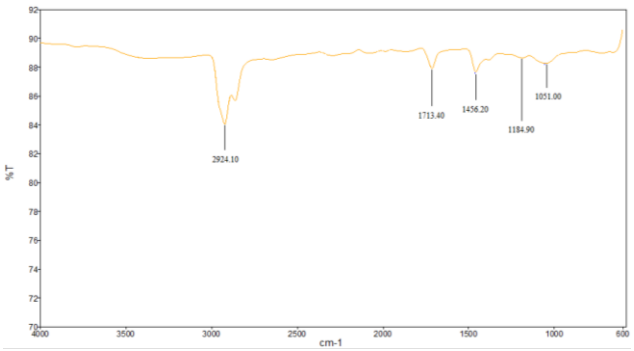

Figure 8 The FTIR spectrum for purified BuBu catalyzed by CS/NC-CRL biocatalyst.

3.4.2 Nuclear Magnetic Resonance (NMR)

^{1}H NMR was utilized to analyze the purified BuBu to match the result in the FTIR. It provides information on the number of different types of protons, obtained by integration of the peak areas. The spectrum of ^{1}H NMR of BuBu was represented in Figure 9. The important peak that corresponded to the structure of BuBu was observed at δ = 3.97 ppm assigned to -CH_2OC=O-. However, an additional peak with a chemical shift, δ=3.54 ppm was consistent with the –CH_2OH. This shows the presence of a trace amount of butanol, hence agrees well with the weak, slightly broad peak at 3200 cm^{-1} in the FTIR spectrum.

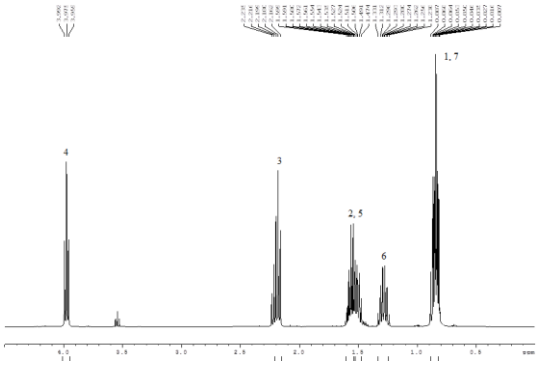

Figure 9 Spectrum of ^{1}H NMR and assignments for butyl butyrate.

4. CONCLUSION

In this study, NC was successfully extracted from raw OPFL and the study found that pure NC appears to be whitish flakes. The morphological characterizations of the extracted NC as well as the raw OPFL were successfully carried out using XRD. The results indicated that the NC from the pretreated OPFL was a good source of NC, with crystallinity index as much as 70%. The RSM-assisted CS/NC-CRL catalyzed esterification showed that the optimum condition that gave the highest percent yield of butyl butyrate at 77.38% ($p < 0.05$) was the use of 5 hrs of reaction at 30˚C using 0.30% (v/v) concentration of the crosslinker ($p < 0.05$).

REFERENCES

[1] Anwar, Z., Gulfraz, M., and Irshad, M. (2014). Agro-industrial lignocellulosic biomass a key to unlock the future bio-energy: A brief review. Jornal of Radiation Research and Applied Sciences. 163-173.

[2] Aljuboori, A.H.R. (2013). Oil Palm Biomass Residue In Malaysia : Availability And Sustainability. International Journal of biomass & renewable. 2(1), 13-18.

[3] Awalludin, M.F., Sulaiman, O., Hashim, R., and Wan Nadhari, W.N.A. (2015). An overview of the oil palm industry in Malaysia and its waste utilization through thermochemical conversion, specifically via liquefaction. Renew Sust Energy Rev. 50, 1469–1484.

[4] Dash, M., Chiellini, F., Ottenbrite, R.M. and Chiellini, E. (2011). Chitosan-A versatile semi synthetic polymer in biomedical applications. Progress in Polymer Science. 36(8), 981–1014.

[5] Elhakeem, M.A.A., Elsayed, A.M. and Alkhulaqi, T.A. (2014). Activity and stability of immobilized Candida rugosa lipase on chitosan coated Fe3O4 nanoparticles in aqueous and organic media. Journal of Advances in Chemistry. 10(3). 2478-2483.

[6] Hung, T. C., Giridhar, R., Chiou, S. H. and Wu, W. T. (2003). Binary immobilization of Candida rugosa lipase on chitosan. Journal of Molecular Catalysis B: Enzymatic. 26, 69-78.

[7] Ju, I. B., Lim, H. W., Jeon, W., Suh, D. J., Park, M. J. and Suh, Y.W. (2011). Kinetic study of catalytic esterification of butyric acid and n-butanol over Dowex 50Wx8-400. Chemical Engineering Journal. 168(1), 293-302.

[8] Marzuki, N.H.C., Mahat, N.A., Huyop, F., Enein, H.Y.A. and Wahab, R.A. (2015). Sustainable production of the emulsifier methyloleate by Candida rugosa lipase nanoconjugates. Food and Bioproducts Processing. 96, 211-220.

[9] Pillai, C.K.S., Paul, W. and Sharma C. P. (2009). Chitin and chitosan polymers: Chemistry, solubility and fiber formation. Progress in Polymer Science. 34(7), 641-678.

[10] Sarbon, N.M., Sandanamsamy, S., Kamaruzaman, S.F.S. and Ahmad, F. (2015). Chitosan extracted from mud crab (Scylla olivicea) shells: physicochemical and antioxidant properties. J Food Sci Technol. 52(7), 4266–4275.

[11] Yahya, M., Lee, H.V., Zain, S. K., and Hamid, S.B.A. (2015). Chemical conversion of palm based lignocellulosic biomass to nanocelullose: review. Polymers Research Journal. 9(4), 3-7.